npg

ORIGINAL ARTICLE

The role of a polyester-based thermoplastic elastomer in the crystallization of an aliphatic polyketone terpolymer

Youngho Eom, Jeongsik Bae and Byoung Chul Kim

The effect of a commercial grade polyester thermoplastic elastomer (HY) on the crystallization behavior of a polyketone terpolymer of ethylene, propylene and carbon monoxide (EPCO) was investigated in terms of shear rate, temperature and blend composition. HY retarded the isothermal crystallization of EPCO in the static state. As the HY content increased, the half-time for the crystallization of the EPCO/HY blends increased, and the cold crystallization temperature (T_c) decreased. In addition, the average value of the Avrami exponent decreased, but the crystallization rate constant increased. The retardation of crystallization could be explained by steric hindrance or a shield effect of the HY phase on the growth of EPCO spherulites at a temperature near the T_c. HY also retarded the crystallization of EPCO in the dynamic state. However, the induction time of the blends was slightly decreased by increasing the magnitude of shear rate up to 10 rad s^{-1}. X-ray diffraction revealed that the introduction of HY had little influence on the crystal structure of EPCO.

INTRODUCTION

The aliphatic terpolymer of ethylene, propylene and carbon monoxide (EPCO) has attracted much attention from polymer engineers and scientists because of its excellent physicochemical properties. Favorable properties such as high tensile strength, high wear resistance, low gas permeability and high chemical resistance give EPCO great potential as an engineering plastic and a barrier packaging material.[1–9] However, control of the temperature to below 240°C is recommended for the melt fabrication process of EPCO because thermal degradation occurs readily at a higher temperature.[10–14] This is a result of residual palladium, the polymerization catalyst, for EPCO, which frequently causes trouble in the melt processing of EPCO because of a very narrow processing window.[1,7] For example, the exceptionally high rate of crystallization in the injection molding process sometimes causes problems such as blockage of the sprue and warping of the resultant products.

It is recognized that most foreign materials lead to a higher crystallization rate of crystalline polymers. However, in addition to improving the notched impact properties, a polyester-based thermoplastic elastomer (HY) retards the crystallization of crystalline EPCO.[15] In this study, we elucidated the retardation mechanism of the crystallization of EPCO by HY by investigating the crystallization behavior of EPCO in the static and dynamic states in terms of the dynamic shearing condition as well as blend composition.
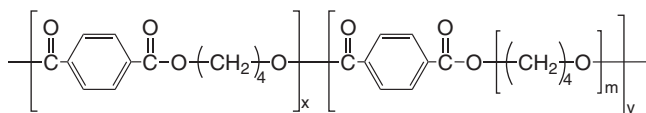
EXPERIMENTAL PROCEDURE

Materials

EPCO (Hyosung Co., Anyang, South Korea) and HY (Hytrel 4069, Dupont, USA) were vacuum dried at 60 °C for 12 h prior to use. EPCO was composed of randomly repeated units of -(CH$_2$-CH$_2$-C=O)- and -(CH$_2$-CH(CH$_3$)-C=O)-, the melt index of which was 60 at 240 °C and 2.16 kg load (ASTM D1238). HY was composed of poly(tetramethylene terephthalate) as a hard segment and poly(oxytetramethylene) glycol as a soft segment, as schematically shown in Scheme 1.[16,17] EPCO and HY were melt mixed in a Haake internal mixer at 240 °C at 80 rpm for 4 min. Blends containing 10, 20, 30 and 40 wt% HY were coded as HY10, HY20, HY30 and HY40, respectively.

Measurement of physical properties

Thermal properties were measured by differential scanning calorimetry (DSC Q20, TA Instruments, New Castle, DE, USA) in a nitrogen atmosphere. For differential scanning calorimetry measurement, the scan rate was 10 °C min^{-1} over a temperature range of −20 to 250 °C. To observe the isothermal crystallization process in the static state, the samples were held at 245 °C for 3 min in differential scanning calorimetry, then they were cooled to the preset temperature (T_i) to bring about isothermal crystallization.

Surface morphology of EPCO/HY blends was observed by scanning electron microscopy (FE-SEM, JSM-6340F, JEOL, Tokyo, Japan). The specimens were fractured in liquid nitrogen. The fractured surface was then etched by formic acid to dissolve the HY phase. The etched surface was sputter-coated with a thin Pt layer to avoid charging. The crystal structure of EPCO, HY and their blends was examined with a wide-angle X-ray diffractometer (WAXD, Rigaku Denki Co., Tokyo, Japan) with Nickel filtered CuKα radiation of 40 kV and 60

Department of Organic and Nano Engineering, Hanyang University, Seongdong-gu, Seoul, Korea
Correspondence: Professor BC Kim, Department of Organic and Nano Engineering, Hanyang University, 222 Wangsimni-ro, Seoul 133-791, Seongdong-gu, Korea.
E-mail: bckim@hanyang.ac.kr
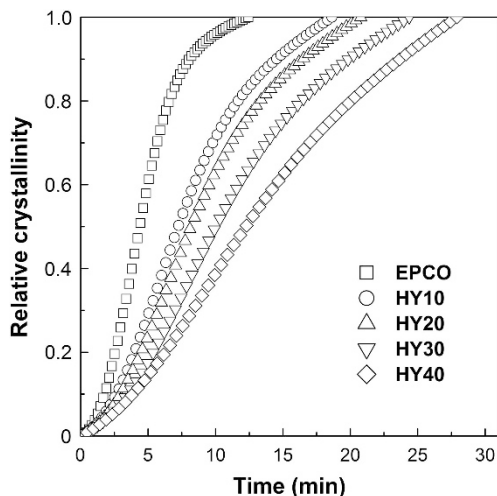
Scheme 1 The chemical structure of Hytrel.

Figure 1 Plots of relative crystallinity versus time for the quiescent isothermal crystallization of EPCO and EPCO/HY blends at 197.5 °C.

Table 1 The half-time of crystallization and the Avrami parameters of EPCO and EPCO/HY blends at various isothermal temperatures

Sample	T_i (°C)	$t_{0.5}$ (min)	n	Kt (× 10^{-2})
EPCO	195	2.5	2.15	9.7
	197.5	4.4	2.12	3.0
	200	8.3	1.98	1.0
HY10	195	4.0	1.97	4.6
	197.5	7.2	1.86	1.7
	200	15.4	1.60	0.9
HY20	195	4.5	1.92	3.8
	197.5	8.2	1.83	1.5
	200	18.8	1.61	1.6
HY30	195	5.0	1.93	3.1
	197.5	10.1	1.78	1.1
	200	21.5	1.67	0.4
HY40	195	5.7	1.83	2.9
	197.5	12.3	1.70	0.9
	200	27.3	1.51	0.4

Abbreviations: EPCO, ethylene, propylene and carbon monoxide; HY, thermoplastic elastomer.

mA. A scanning experiment was carried out on the equator over the 2θ range of 5–50° at a scan speed of 7° min^{-1}.

Dynamic mechanical properties of EPCO and HY were measured by dynamic mechanical analysis (DMA Q800, TA Instruments) at a rate of 5 °C min^{-1} with a load frequency of 1 Hz under a nitrogen atmosphere. Rheological properties were measured by an Advanced Rheometric Expansion System (TA Instruments) at 240 °C in a nitrogen atmosphere. A parallel plate geometry, the diameter and gap of which were 25 and 0.8 mm respectively, was adopted. The strain level was adjusted to 5% as indicated by preliminary tests. The Advanced Rheometric Expansion System specimen was prepared by compression molding to minimize residual stress. Prior to measurement, the melt was kept between the plates for 4 min to fully relax residual stresses. To observe the isothermal crystallization process under dynamic shear conditions, a time sweep measurement was carried out at 1 and 10 rad s^{-1} until the storage modulus (G') reached the ceiling value.

RESULTS AND DISCUSSION

The relative crystallinity (X_t) with crystallization time (t) is calculated by Equation (1)[18]

$$X_t = \frac{\int_{t_0}^{t} (dH/dt)dt}{\int_{t_0}^{t_\infty} (dH/dt)dt} \qquad (1)$$

in which dH/dt is the rate of heat evolution and t_0 and t_∞ are the times at which crystallization process begins and ends, respectively. Figure 1 shows the X_t of EPCO and EPCO/HY blends versus time at 197.5 °C. The half-time of crystallization ($t_{0.5}$) of EPCO and the blends at the isothermal crystallization temperature (T_i) obtained from Figure 1 is given in Table 1. The $t_{0.5}$ of the blends increases with increasing HY content. This indicates that HY reduces the crystallization rate of EPCO.

The cooling and subsequent heating differential scanning calorimetry scans of EPCO, HY and their blends are shown in Figures 2a and b, respectively. As a rule, the incorporation of a foreign material increases the crystallization rate of a crystalline polymer by causing
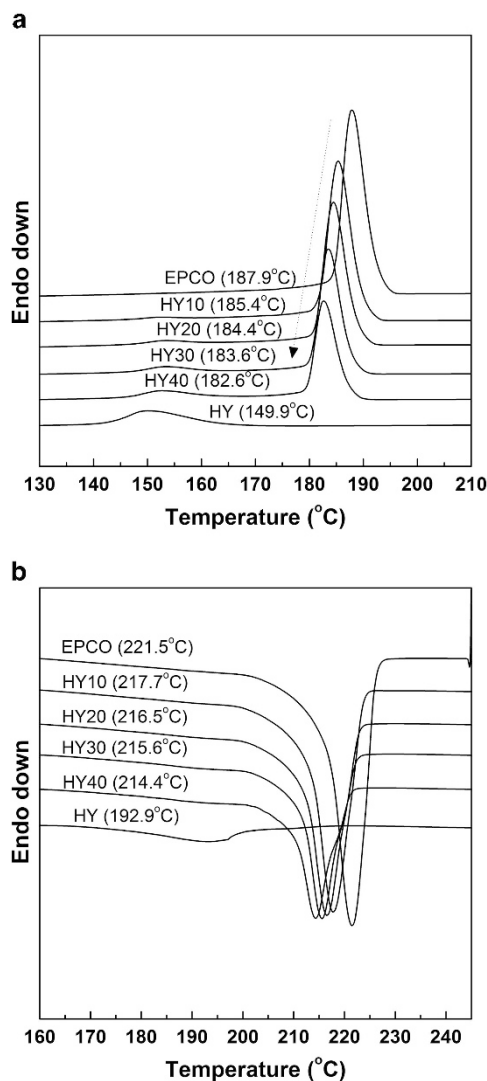

Figure 2 DSC (**a**) cooling and (**b**) heating scan thermograms of EPCO, HY and EPCO/HY blends.

heterogeneous nucleation because the foreign material mostly has a role as a nucleating agent. Hence, heterogeneous crystallization at an interface leads to an increase in the T_c of a blend.[18–22] As reported, HY is a foreign material because it has little miscibility with EPCO.[15] This can be confirmed by the wide-angle X-ray diffractometer patterns of the neat polymers and their blends. In Figure 3, EPCO obviously shows strong peaks of β forms at 22, 25 and 28°, representing the (110), (111) and (210) planes, respectively.[23] The blends show the unique EPCO peaks as well at the same scattering angle without generating new diffraction peaks. Therefore, the accelerated crystallization of EPCO is expected in principle. However, in reality, HY decelerates the crystallization of EPCO as evidenced by a decrease in

the T_c of the immiscible blends with increasing HY content. This suggests that crystallization as well as nucleation of the blends occurs only in the neat EPCO phase without any contribution from the amorphous HY phase.[24] However, the solvent-etched morphology of the blends in Figure 4 shows that the HY domains are widely dispersed in the form of droplet-like domains in the EPCO matrix. As a result, these immiscible HY domains seem to physically disturb the crystal growth of EPCO along the path of spherulite development. This results in a decreased crystal size and perfectness, which corresponds to the reduction of the T_m of the blends as shown in Figure 2b.
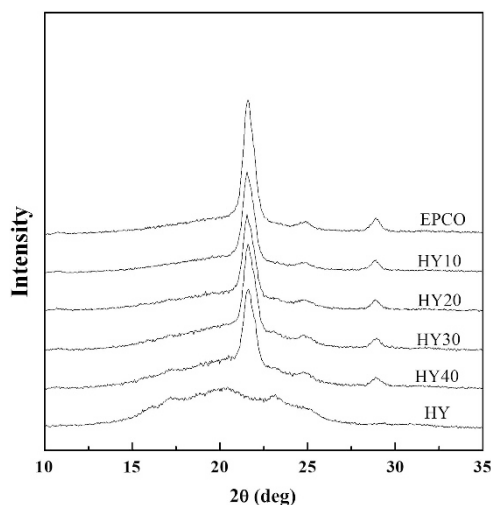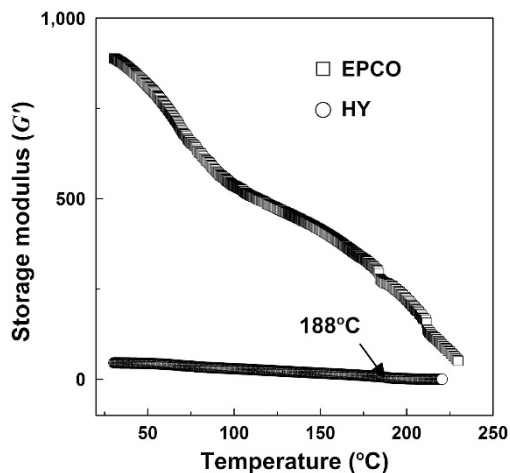

**Figure 3** WAXD profiles of EPCO, HY and EPCO/HY blends.
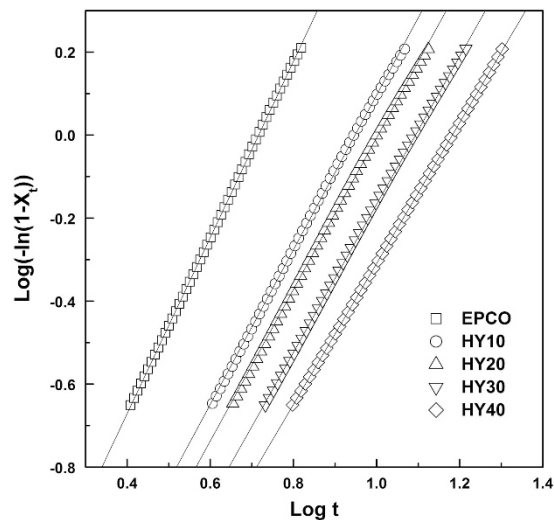
Figure 5 Avrami plots for the quiescent isothermal crystallization of EPCO and EPCO/HY blends at 197.5 °C.
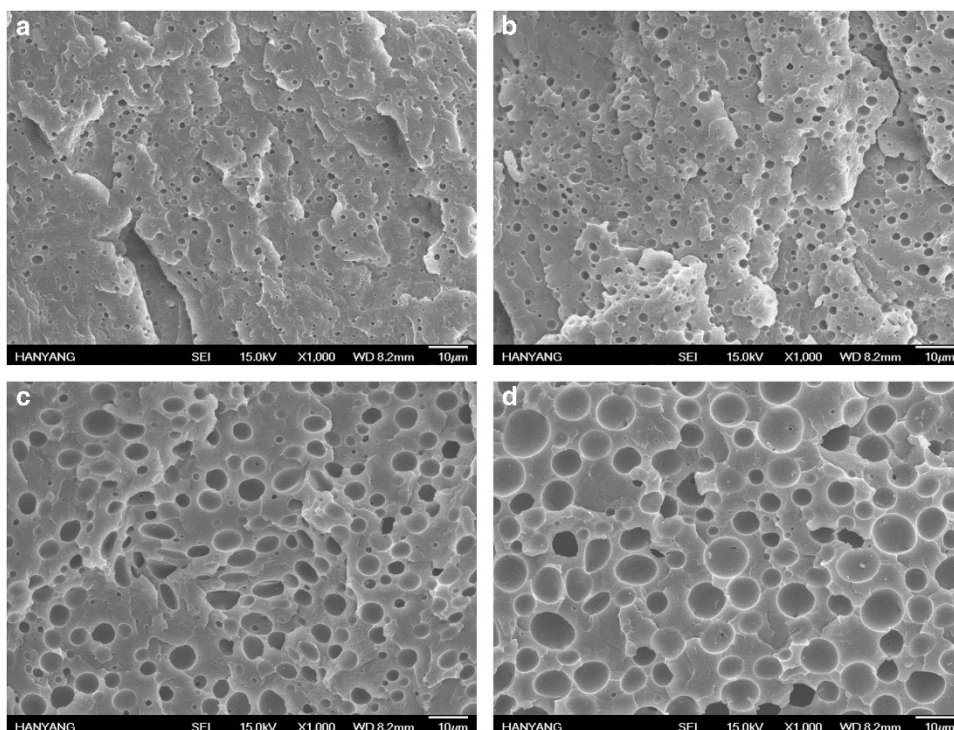
Figure 4 The solvent etched morphology of (**a**) HY10, (**b**) HY20, (**c**) HY30 and (**d**) HY40, respectively. HY was extracted with formic acid.

Figure 6 The variation of the storage modulus (G') of EPCO and HY with increasing temperature. The marked temperature on the graph is the T_c of EPCO.
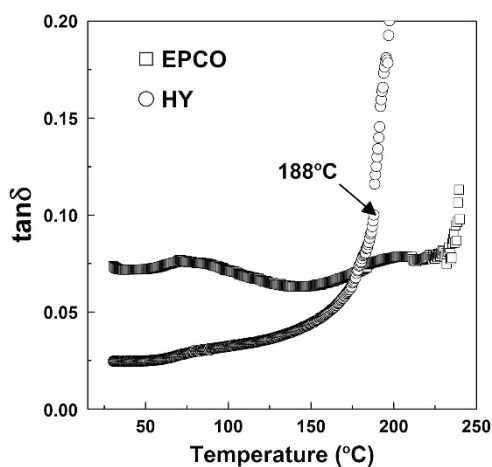

Figure 7 The variation of tanδ for EPCO and HY with increasing temperature. The marked temperature on the graph is the T_c of EPCO.

**Table 2 The induction time of EPCO and EPCO/HY blends under the dynamic condition at 197°C**

Sample	Induction time (s)	
	ARES (197°C)	
	1 rad s^{-1}	*10 rad s^{-1}*
EPCO	225.7	213.3
HY10	262.2	256.0
HY20	317.3	301.8
HY30	387.1	374.7
HY40	453.8	444.5

Abbreviation: ARES, Advanced Rheometric Expansion System.

Figure 5 shows the Avrami plots of EPCO and its blends at 197.5 °C. The Avrami exponent (n) and crystallization rate constant (K_t) obtained at different T_is are listed in Table 1. The n is a measure of the dimensionality of the spherulite growth and the average values for
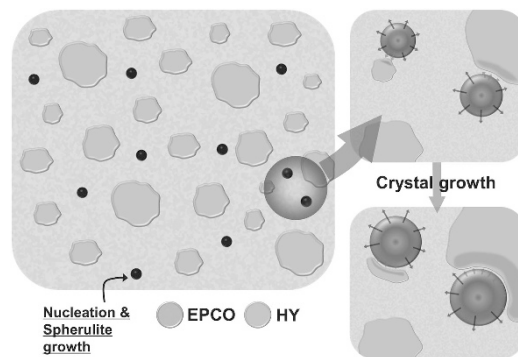
Scheme 2 The retardation mechanism of the crystallization of EPCO by the incorporation of HY in the blend phase. A full color version of this figure is available at *Polymer Journal* online.
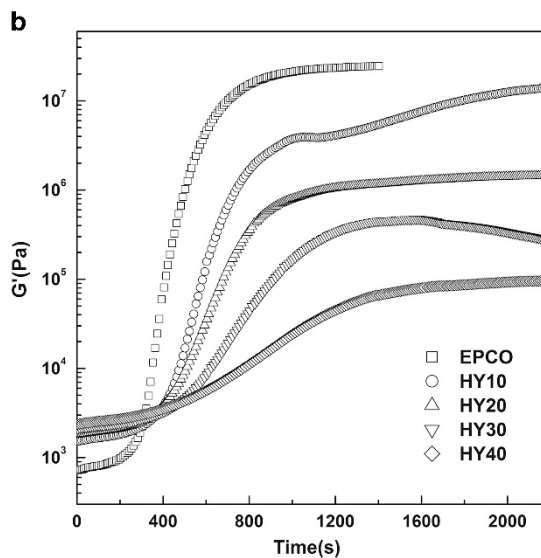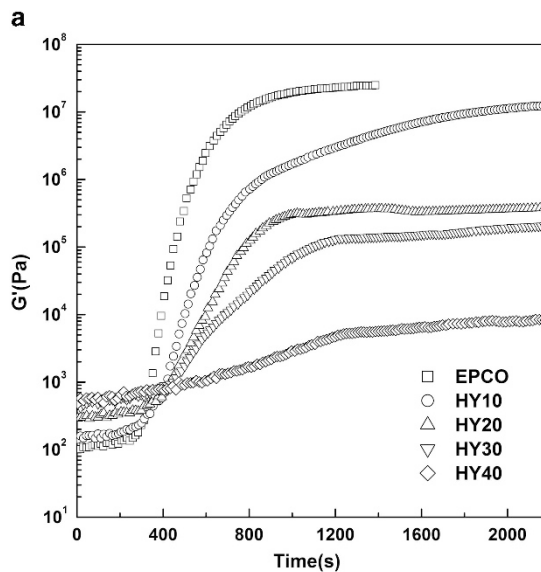
Figure 8 Shear-induced isothermal crystallization of EPCO and EPCO/HY blends at 197 °C and (**a**) 1 rad s^{-1} and (**b**) 10 rad s^{-1}, respectively.

each sample at several T_i decrease from 2.08 to 1.68 with an increasing HY content, which indicates the reduced dimensionality of the EPCO spherulites. In addition, as the HY content increases the K_t values decrease, which further verifies the retardation of the crystallization of EPCO.

The variation of storage moduli (G') of two polymers with temperature is plotted in Figure 6. HY gives much lower values of G' than EPCO over the temperature range shown, indicating a very low melt viscosity of HY. Furthermore, the phase character of HY and EPCO at T_c can be verified by the variation of loss tangent (tanδ) in Figure 7. A greater value of tanδ indicates a higher liquidity of the samples.[25] HY gives greater tanδ than EPCO above 188 °C, T_c of EPCO, which means a higher liquid character of the HY phase than for the EPCO matrix over the temperature range of crystallization. Hence, the liquid-like HY phase easily shields the EPCO spherulites during the crystal growth, as illustrated in Scheme 2.[26,27] In addition, the two components may be slightly miscible to a limited extent because both polymers contain carbonyl groups in the main chain. As a consequence, it is expected that the crystal growth of EPCO in the blend was retarded because the EPCO chains have to displace the HY moiety from the spherulite surface during the crystal growth process.

The effect of the shear stress on the crystallization of polymeric systems is evaluated by dynamic rheological measurement at a given temperature. This can be done by tracing the variation of G' with time at the temperature. Figure 8 shows the variation of the G' of the EPCO and EPCO/HY blends with time at different frequencies at 197 °C. G' increases very slowly during the early stages. This period is referred as the induction time for crystallization. The induction period is defined as the stage when randomly entangled polymer chains transform to a regularly aligned lattice. Then, an abrupt increase of G' follows because the homogeneous melt becomes a heterogeneous system with the formation and growth of crystallites. The induction time of EPCO and its blends at different frequencies are given in Table 2. The induction time is notably increased with an increasing HY content at all frequencies considered, indicating that HY still reduces the crystallization rate of EPCO even in the dynamic state.

It is noteworthy that the induction time of the blends is slightly decreased with an increase in the shear rate. In most cases, shear-induced crystallization takes place under dynamic conditions in polymer systems.[18,19,21] However, when shear stress is applied to the EPCO/HY blends, it may be almost concentrated on the easily deformable HY domains because of the lower viscosity and Newtonian character, as previously mentioned. Then, the HY phase rapidly dissipates the large stresses. The cavity on the interface is direct evidence for the stress-dissipation of the HY elastomer.[15] Hence, the shear rate has little effect on the crystallization behavior of the EPCO/HY blends.

CONCLUSION

The crystallization behavior of the EPCO/HY blends in the static and dynamic states revealed that HY retarded the crystallization of EPCO without changing its crystal structure. The large difference in the elastic moduli of the two polymers at the crystallization temperature was the principal reason for the retardation process. This is a somewhat unexpected result. However, this result may be effectively utilized in the design of injection molding processes for EPCO by widening the processing window.

1 Drent, E. & Budzelaar, P. H. M. Palladium-catalyzed alternating copolymerization of alkenes and carbon monoxide. *Chem. Rev.* **96**, 663–681 (1996).
2 Jawad, S. A., Abu-Surrah, A. S., Maghrabi, M. & Khattari, Z. Dielectric behavior of alternating ethylene, propylene, and carbon monoxide Co- and terpolymers via impedance spectroscopy. *J. Appl. Polym. Sci.* **123**, 2020–2026 (2012).
3 Kato, A., Nishioka, M., Takahashi, Y., Suda, T., Sawabe, H., Isoda, A., Drozdova, O., Hasegawa, T., Izumi, T., Nagata, K., Hikasa, S., Iwabuki, H. & Asano, A. Phase separation and mechanical properties of polyketone/polyamide polymer alloys. *J. Appl. Polym. Sci.* **116**, 3056–3069 (2010).
4 Lagaron, J. M., Vickers, M. E., Powell, A. K. & Davidson, N. S. Crystalline structure in aliphatic polyketones. *Polymer* **41**, 3011–3017 (2000).
5 Lommerts, B. J., Klop, E. A. & Aerts, J. Structure and melting of perfectly alternating ethylene carbon-monoxide copolymers. *J. Polym. Sci. Pol. Phys.* **31**, 1319–1330 (1993).
6 Lopez-Rubio, A., Gimenez, E., Gavara, R. & Lagaron, J. M. Gas barrier changes and structural alterations induced by retorting in a high barrier aliphatic polyketone terpolymer. *J. Appl. Polym. Sci.* **101**, 3348–3356 (2006).
7 Sommazzi, A. & Garbassi, F. Olefin carbon monoxide copolymers. *Prog. Polym. Sci.* **22**, 1547–1605 (1997).
8 Zhang, Y. C., Broekhuis, A. A., Stuart, M. C. A. & Picchioni, F. Polymeric amines by chemical modifications of alternating aliphatic polyketones. *J. Appl. Polym. Sci.* **107**, 262–271 (2008).
9 Zuiderduin, W. C. J., Huetink, J. & Gaymans, R. J. Rigid particle toughening of aliphatic polyketone. *Polymer* **47**, 5880–5887 (2006).
10 Chiantore, O., Lazzari, M., Ciardelli, F. & DeVito, S. Pyrolysis and thermal degradation of ethylene carbon monoxide alternating copolymers. *Macromolecules* **30**, 2589–2597 (1997).
11 Chien, J. C. W. & Zhao, A. X. Thermolysis of alternating ethylene carbon-monoxide copolymer. *Polym. Degrad. Stabil.* **40**, 257–261 (1993).
12 Conti, G. & Sommazzi, A. Thermal-degradation of polyketones - vibrational spectroscopy studies. *J. Mol. Struct.* **294**, 275–278 (1993).
13 De Vito, S., Ciardelli, F., Ruggeri, G., Chiantore, O. & Moro, A. Thermal degradation of ethylene carbon monoxide alternating copolymer under inert atmosphere. *Polym. Int.* **45**, 353–365 (1998).
14 Gooden, R., Davis, D. D., Hellman, M. Y., Lovinger, A. J. & Winslow, F. H. Effects of elongation on the photochemistry of Poly[Ethylene-Co-(Carbon Monoxide)]. *Macromolecules* **21**, 1212–1217 (1988).
15 Bae, J. K. B. C. The rheological design of aliphatic polyketone terpolymer blendswith polyester thermoplastic elastomer. *Macromol. Res.* **22**, 1165–1169 (2014).
16 Kalfoglou, N. K. Thermomechanical studies of semicrystalline polyether-ester copolymers - effect of thermal, mechanical, and solvent treatment. *J. Appl. Polym. Sci.* **21**, 543–554 (1977).
17 Kwak, S. Y. & Nakajima, N. Morphology formation in mixing of copolyester thermoplastic elastomer (Hytrel) with poly(vinyl chloride) and nuclear magnetic resonance relaxation study on solid structures of the mixture. *Macromolecules* **29**, 3521–3524 (1996).
18 Nam, Y., Shim, K. B., Kim, S. H. & Kim, Y. C. Effect of silica nanoparticle on the quiescent and the shear induced crystallization behaviors of poly(trimethylene terephthalate). *Polym. J.* **36**, 519–530 (2004).
19 Chae, D. W. & Kim, B. C. Physical properties of isotactic poly (propylene)/silver nanocomposites: dynamic crystallization behavior and resultant morphology. *Macromol. Mater. Eng.* **290**, 1149–1156 (2005).
20 Chae, D. W. & Kim, B. C. Effects of introducing silica particles on the rheological properties and crystallization behavior of poly(ethylene terephthalate). *J. Mater. Sci.* **42**, 1238–1244 (2007).
21 Chae, D. W., Shim, K. B. & Kim, B. C. Effects of silver nanoparticles on the dynamic crystallization and physical properties of syndiotactic polypropylene. *J. Appl. Polym. Sci.* **109**, 2942–2947 (2008).
22 Lee, S. J., Hahm, W. G., Kikutani, T. & Kim, B. C. Effects of clay and POSS nanoparticles on the quiescent and shear-induced crystallization behavior of high molecular weight poly(ethylene terephthalate). *Polym. Eng. Sci.* **49**, 317–323 (2009).
23 Waddon, A. J. & Karttunen, N. R. Poly(olefin ketone)s: comparison of the effects of CH3 and CH3CH2 side groups on the crystal structure. *Macromolecules* **35**, 4003–4008 (2002).
24 Bartczak, Z., Galeski, A. & Krasnikova, N. P. Primary nucleation and spherulite growth-rate in isotactic polypropylene polystyrene blends. *Polymer* **28**, 1627–1634 (1987).
25 Chae, D. W., Kim, M. H. & Kim, B. C. Temperature dependence of the rheological properties of poly(vinylidene fluoride)/dimethyl acetamide solutions and their electro-spinning. *Korea-Aust. Rheol. J.* **22**, 229–234 (2010).
26 Bartczak, Z., Galeski, A. & Martuscelli, E. Spherulite growth in isotactic polypropylene-based blends - energy and morphological considerations. *Polym. Eng. Sci.* **24**, 1155–1165 (1984).
27 Martuscelli, E. Influence of composition, crystallization conditions and melt phase-structure on solid morphology, kinetics of crystallization and thermal-behavior of binary polymer polymer blends. *Polym. Eng. Sci.* **24**, 563–586 (1984).